THz MIMO Channel Characterization for Wireless Data Center-Like Environment

Chia-Lin Cheng, Seun Sangodoyin, and Alenka Zajić
Georgia Institute of Technology, Atlanta, GA 30332 USA

***Abstract*— In this paper, we present the measurement setup and results obtained from a Terahertz (THz) Multiple-Input-Multiple-Output (MIMO) channel sounding experiment conducted in a data center-like environment. These measurements were conducted in Line-of-sight (LoS) and Obstructed-line-of-sight (OLoS) scenarios with cables of varying thickness serving as obstruction. The modeling of pathloss, shadowing gain, RMS delay spread, and signal amplitude statistics have been presented. The results provided in this paper are the starting point for a realistic performance evaluations of THz communications in wireless data center environments.**

I. Introduction

Data centers have become a crucial component for cloud computing and storage [1], where reliable and high-speed connectivity is required. Traditionally, metal wires and optical waveguides have been used for transmission in data centers, however, due to their increasing assembly and maintenance cost, service time, and decreasing cooling efficiency, wireless communication is being considered as an alternative [2]. A key challenge for wireless data centers is the demand for ultra high data rate. Terahertz (THz) frequencies can be used to achieve the required data rates and facilitate wireless data centers. To address this challenge, understanding propagation mechanisms in data center environments are necessary. The first step in that direction is presented in [3], where characterization of single-input single-output THz channels for wireless data centers has been presented. In contrast, this paper presents the characterization of THz wireless channels at 300-312 GHz in a Line-of-sight (LoS) scenario and Obstructed-line-of-sight (OLoS) scenario with cables serving as obstruction for the application of wireless data center using a *virtual* Multiple-Input-Multiple-Output (MIMO) antenna array configuration. Modeling of pathloss, shadowing gain, RMS delay spread and signal amplitude statistics have been presented in this work. The remainder of this paper is organized as follows. Section II describes the measurement setup and propagation scenarios. Section III presents data evaluation results. Section IV provides concluding remarks.

II. Measurement Setup and Scenarios

The propagation channel measurements were conducted in the EMC^2 Lab on the campus of the Georgia Institute of Technology, Atlanta, GA using a data center-like environment (as shown in Fig. 1). These measurements were performed

This work has been supported, in part, by NSF grant 1651273. The views and findings in this paper are those of the authors and do not necessarily reflect the views of NSF.

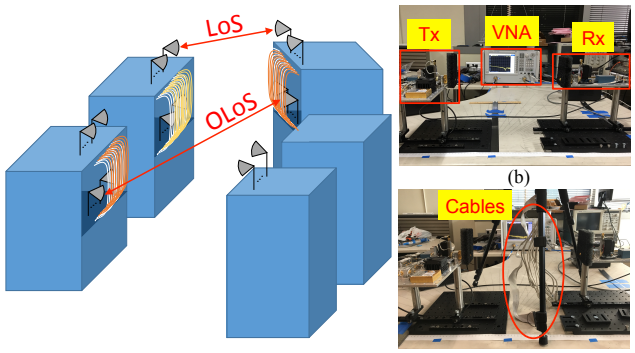

Fig. 1. (a) LoS and OLoS links in a wireless data center, (b) LoS measurement setup, (c) OLoS measurement setup.

with a N5224A PNA vector network analyzer (VNA) and VDI transceivers (Tx210/Rx148) over a bandwidth of 12 GHz (subdivided into 801 frequency tones). The vertically polarized horn antenna used at the $T_{\rm x}$ and $R_{\rm x}$ ends has a gain of approximately 23 dBi and a half-power beamwidth (HPBW) at around 10°. More details on the measurement setup can be found in [4]. Measurement configuration for LoS and OLoS are presented in Figs. 1 (b) and (c). Measurements were recorded at $T_{\rm x}$-$R_{\rm x}$ separation distance, d=40 to 100 cm in 10 cm increments. To replicate an OLoS scenario in which cables are expected to serve as obstructions, cable clusters with 3 different thickness sizes were positioned between $T_{\rm x}$ and $R_{\rm x}$ thereby creating different shadowing realizations. In order to extract small-scale fading statistics, we conduct 4×4 MIMO measurement using a virtual uniform linear array (ULA) configuration [5] with a step size of 2 mm between antenna array elements, thereby providing a total of 16 channel realizations.

III. Results and Analysis

A. Pathloss and Shadowing Gain Modeling

We modeled the pathloss using the floating-intercept (FI, alpha-beta, or 3GPP) equation,

$$PL^{FI}(d) = \alpha + 10 \cdot \beta \cdot \log_{10}\left(\frac{d}{d_0}\right) + X_{\sigma}^{\rm FI}, d \geq d_0, \quad (1)$$

where α (dB) is the floating intercept, β is the pathloss exponent (PLE), and $X_{\sigma}^{\rm FI}$ is the Gaussian-distributed shadowing gain with standard deviation σ. The measured mean path loss and the FI models for the LoS and OLoS scenarios, as well as the statistical distribution fit for the OLoS shadowing gain are presented in Figs. 2 (a) and (b), respectively. All parameters

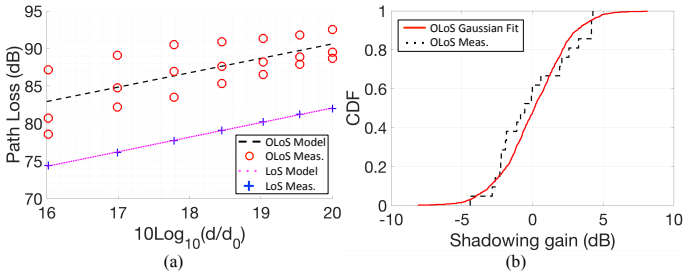

Fig. 2. (a) Pathloss models for LoS and OLoS scenarios at d=40-100 cm, (b) Gaussian-distributed CDF of shadowing gain (X_{σ}^{FI}) for OLoS scenario.

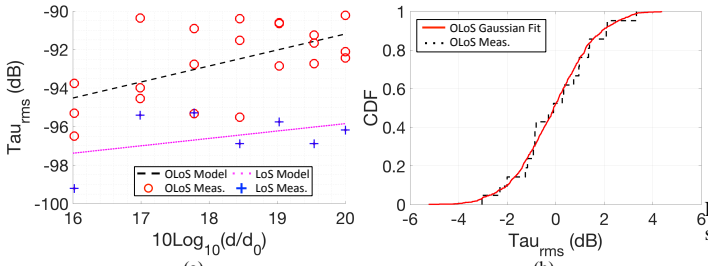

Fig. 3. (a) Measured and modeled τ_{rms} for LoS and OLoS scenarios at d=40-100 cm, (b) Gaussian-distributed CDF of L_{σ} for OLoS scenario.

from (1) are summarized in Table I. It can be observed that LoS and OLoS scenarios have similar PLEs at about 1.9, which are close to the free-space PLE of 2, however, α (dB) and the shadowing gain varies significantly in both scenarios.

TABLE I

PATHLOSS MODEL PARAMETERS.

	α (dB)	β (PLE)	Xσ (dB)
LoS	43.2	1.94	0.06
OLoS	52.2	1.92	2.6

B. Delay Dispersion Modeling

The delay dispersion in multipath environments can be captured by the rms delay spread, τ_{rms}. We found the τ_{rms} to be lognormally distributed with the logarithmic equivalent of the first and second moments presented as $\mathcal{N}(-96.8\mathrm{dB}, -102.1\mathrm{dB})$ and $\mathcal{N}(-92.2\mathrm{dB}, -96.2\mathrm{dB})$ for LoS and OLoS, respectively. We also found τ_{rms} to exhibit a monotonic dependence on distance, hence we propose model as:

$$\tau_{rms}(d) = G_{T_0} + 10 \cdot \epsilon \cdot \log_{10}\left(\frac{d}{d_0}\right) + L_{\sigma}, d \geq d_0, \quad (2)$$

where G_{T_0} (dB) is the intercept, ϵ is the slope parameter, and L_{σ} is the Gaussian-distributed random variable with standard deviation σ. Fig. 3(a) presents the measured and modeled τ_{rms} (dB) for LoS and OLoS scenarios, and Fig. 3(b) presents the statistical distribution fit of L_{σ}. Values of these parameters are summarized in the Table II.

TABLE II

RMS DELAY MODEL PARAMETERS.

	G_{T0} (dB)	Є	Lσ (dB)
LoS	-103.5	0.38	1.1
OLoS	-107s.8	0.83	1.6

C. Signal Amplitude Statistics

In this work, we have found that signal amplitude distribution can be modeled using m-Nakagami distribution. With an ensemble of the shadowing points and distances measured, we have found the m-parameter of the Nakagami distribution to be a random variable and have therefore modeled its logarithmic equivalent using a truncated Gaussian distribution denoted by $m-$ $(T_N(\mu_m(dB), \sigma_m^2(dB))$ with the probability density function (PDF) shown in Fig. 4.

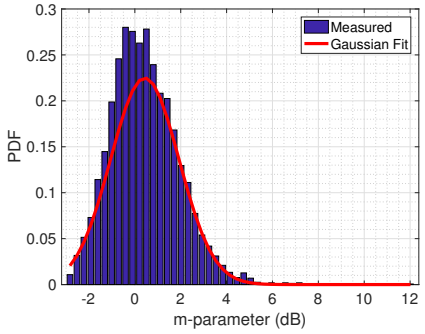

Fig. 4. PDF of the m-parameter (dB) using an ensemble over distances and shadowing points.

We have also found the mean (μ_m) and standard deviation (σ_m) values over the aforementioned ensemble to show a monotonic dependency over the excess delay bins (τ_k) of the power-delay profiles at each measured location. A linear model for μ_m and σ_m as a function of delay bin (τ_k) are shown in (3) and (4).

$$\mu_m(\tau_k) = A - \frac{1}{B}\tau_k, \quad (3)$$

$$\sigma_m(\tau_k) = C - \frac{1}{D}\tau_k, \quad (4)$$

where the unit of τ_k is in nanosecond. Values of parameters A, B, C, and D are summarized in Table III.

TABLE III

SIGNAL AMPLITUDE STATISTICS.

	A	B	C	D
LoS	1.241	390.6	0.437	1479.6
OLoS	1.244	149.5	0.541	100.9

IV. CONCLUSIONS

We conducted a measurement campaign in a data center-like environment at THz frequencies with a multi-antenna setup. Channel parameters such as pathloss, shadowing gain, RMS delay spread, and signal amplitude statistics were provided in this paper.

REFERENCES

[1] Y. Cui, H. Wang, X. Cheng, and B. Chen, "Wireless data center networking," *IEEE Wireless Communications*, vol. 18, no. 6, pp. 46–53, December 2011.

[2] T. Chen, X. Gao, and G. Chen, "The features, hardware, and architectures of data center networks: A survey," *Journal of Parallel and Distributed Computing*, vol. 96, pp. 45 – 74, 2016.

[3] C.-L. Cheng and A. Zajić, "Characterization of 300 ghz wireless channels for rack-to-rack communications in data centers," in *2018 IEEE 29th Annual International Symposium on Personal, Indoor and Mobile Radio Communications (PIMRC)*, Sep. 2018, pp. 194–198.

[4] S. Kim and A. Zajić, "Characterization of 300-ghz wireless channel on a computer motherboard," *IEEE Transactions on Antennas and Propagation*, vol. 64, no. 12, pp. 5411–5423, Dec 2016.

[5] S. Sangodoyin, V. Kristem, A. F. Molisch, R. He, F. Tufvesson, and H. M. Behairy, "Statistical Modeling of Ultrawideband MIMO Propagation Channel in a Warehouse Environment," *IEEE Transactions on Antennas and Propagation*, vol. 64, no. 9, pp. 4049–4063, Sept 2016.